

## ORIGINAL RESEARCH ARTICLE

# Automatic distal radius fracture detection and classification using deep convolutional neural network with radiological images

Iffath Misbah<sup>1,\*</sup>, Aadithiyar Sekar<sup>1</sup>, Sathish Muthu<sup>2</sup>, C. Prajitha<sup>3</sup>, Girinivasan Chellamuthu<sup>4</sup>, Munis Ashraf<sup>4</sup>, Mahalakshmi<sup>5</sup>

<sup>1</sup> Department of Radiology, Saveetha Medical College and Hospital, Saveetha Institute of Medical and Technical Sciences (SIMATS) Saveetha University, Chennai 602105, India

<sup>2</sup> Department of Orthopaedics, Government Medical College & Hospital, Karur 639004, India

<sup>3</sup> Department of Electronics and Communication Engineering/Centre for Interdisciplinary Research, Karpagam Academy of Higher Education, Coimbatore 641021, India

<sup>4</sup> Department of Orthopaedics, Saveetha Medical College and Hospital, Saveetha Institute of Medical and Technical Sciences (SIMATS) Saveetha University, Chennai 602105, India

<sup>5</sup> Department of Computer Science and Engineering, R.L. Jalappa Institute of Technology, Doddaballapur 561203, India

\* Corresponding author: Iffath Misbah, iffathmisbahcp@gmail.com

## ABSTRACT

Distal radius fractures (DRF) are among the most common fractures and are often treated surgically. The accuracy and effectiveness of the surgical procedures greatly depend on the correct classification of distal radius fractures. Wrist fractures are the most commonly misclassified because of the wrist bone's complex anatomical structure, including several different bones. Thus, it is evident that models based on machine learning (ML) and artificial intelligence (AI) are required, with an emphasis on making them user-friendly for everyday clinical practice. Hence, this study proposes the Deep Convolutional Neural Network-based Distal Radius Fracture Classification Model (DCNN-DRFCM) to diagnose DRFs using anteroposterior and lateral wrist radiographs. The goal of this work is to develop an artificial intelligence system that can learn to utilize X-ray pictures to correctly diagnose distal radius fractures with a small amount of information. Labelling assessments with fractures and overlaying fracture masks generates images that may be used for testing and training segmentation and classification methods. The DCNN model analyzed DRF based on three views: lateral, anteroposterior, and lateral and anteroposterior views. The experimental outcomes demonstrate that the recommended model increases the classification accuracy rate of 99.3%, sensitivity rate of 96.5%, specificity rate of 97.8%, and F1-score rate of 95.6% and reduces the error rate of 11.2% compared to other popular approaches.

**Keywords:** distal radius fracture; classification; deep convolutional neural network; radiological images; classification; artificial intelligence

## ARTICLE INFO

Received: 5 March 2024  
Accepted: 26 March 2024  
Available online: 30 May 2024

## COPYRIGHT

Copyright © 2024 by author(s).  
Journal of Autonomous Intelligence is published by Frontier Scientific Publishing. This work is licensed under the Creative Commons Attribution-NonCommercial 4.0 International License (CC BY-NC 4.0).  
<https://creativecommons.org/licenses/by-nc/4.0/>

## 1. Introduction

Distal radius fractures at the wrist are the most common upper extremity fractures<sup>[1]</sup>. Consequently, they make up many of the injuries seen in clinics and emergency departments worldwide. Wrist injuries affect tens of millions of individuals annually worldwide<sup>[2]</sup>. X-ray imaging, which has been used for over a century, is still a common mode of diagnosis<sup>[3]</sup>. Diagnosis of distal radius fractures using X-rays is crucial for treatment purposes. The radiographic features of the fracture pattern are one of the parameters that determine the precise course of treatment when a diagnosis has been

established<sup>[4]</sup>. Immobilization in a cast, reduction in and casting and various internal fixation procedures are all possible treatment options<sup>[5]</sup>. The cornerstone of the therapy includes bringing the fracture components back into proper alignment and keeping them there until sufficient healing has taken place<sup>[6]</sup>. Prognosis is more likely to be negatively impacted in older individuals if fractures are not treated promptly, mainly because of their diminished body function and low physical fitness<sup>[7]</sup>. This has increased the interest in reliable augmentation tools for automatic fracture identification<sup>[8]</sup>.

Despite recent advances in artificial intelligence (AI) surpassing orthopaedics professionals in automated fracture detection, deep learning of convolutional neural networks (CNNs) continues to require large amounts of data (1000 images or more) to increase diagnostic accuracy<sup>[9]</sup>. Misdiagnoses may cause unnecessary suffering and financial losses; however, machine learning can streamline and improve the diagnosing of distal radius fractures from X-ray images<sup>[10]</sup>. To solve the diagnostic issues, CNNs learn discriminating features from the pixel information of large-scale datasets<sup>[11]</sup>. The artificial intelligence model relied on a convolutional neural network (CNN), a category of DL architecture that uses repeated convolution operations on a picture to extract feature<sup>[12]</sup>. Feeding an input image into the model's learnt filters may identify which visual features are most important for the output image<sup>[13]</sup>. Training supervised convolutional neural network (CNN) models often requires massive volumes of labelled data. Parameter optimization and interval validations were done using the validation data set<sup>[14]</sup>. Using test data sets that the trained model had never seen before, researchers looked for symptoms of fractures in radiographs of young people's wrists<sup>[15]</sup>. One way to describe the challenge of fracture identification in vision-based models is as follows: using fracture characteristics to appropriately categorize radiography images into fracture and non-fracture classes<sup>[16]</sup>. Because of their capacity to highlight the apparent fracture site, the radiologist can more readily relate to and use the findings of object identification and segmentation in clinical practice, in contrast with image classification, which initially does not provide spatial information<sup>[17]</sup>.

The key contribution of the article is

- Designing the Deep Convolutional Neural Network-based Distal Radius Fracture Classification Model (DCNN-DRFCM) to diagnose DRFs using anteroposterior and lateral wrist radiographs.
- Evaluating the mathematical model of Deep Convolutional Neural Networks for classifying the fracture and non-fracture of DRFs.
- The numerical findings have been employed, and the suggested DCNN-DRFCM model enhances the sensitivity, accuracy, F1-score, specificity and reduced error ratio compared to existing approaches.

The remainder of the article is pre-organized: section 2 discourses the related survey, section 3 suggests the DCNN-DRFCM, section 4 reflects the findings, and section 5 concludes the research article.

## 2. Related study

Hardalaç et al.<sup>[18]</sup> suggested the ensemble models called wrist fracture detection-combo (WFD-C). Utilizing DL on wrist X-ray pictures, this research hopes to identify fractures and aid doctors in diagnosing them, especially in emergencies. The WFD-C model achieved the best detection performance out of 26 fracture detection models, with an average precision (AP50) of 0.8639. As part of the continuing collaboration project designated 071813 with Huawei, Gazi University, and Medskor, the Huawei Turkey R&D Center helps this work.

Hrzić et al.<sup>[19]</sup> proposed the YOLOv4 method for Fracture Detection in Paediatric Wrist Radiographs. There was a substantial difference between the four radiologists and the YOLO 512 Anchor model-AI, the top-execution YOLOv4-based approach (Radiologist mean AUC-ROC =  $0.831 \pm 0.075$ , AI AUC-ROC = 0.965). Moreover, the author demonstrated that the AI model considerably enhanced the performance of

three out of five radiologists. The results are supported by a comprehensive dataset of 19,700 X-ray pictures of children.

Meena and Roy<sup>[20]</sup> recommended Deep Supervised Learning (DSL) for Bone Fracture Detection from Radiological Images. Fracture identification is an area where CNN-based models, particularly InceptionNet and XceptionNet, excel, according to this study's findings. This research aimed to demonstrate how DL is used in medical imaging to aid radiologists in diagnosing accurately. The author has covered the history, present, and future of deep learning (DL) in bone imaging and its difficulties and obstacles.

Malik et al.<sup>[21]</sup> discussed the Hand-Crafted and Deep Feature Fusion and Selection and Wolf Optimization Algorithm (HC-DFFS-WOA). The method for fractured elbow classification is based on the whale optimization approach. Handcrafted features, like the histogram of oriented gradient (HOG) and the local binary pattern (LBP), are retrieved from the input photos. The best features are chosen utilizing principal component analysis (PCA) and then sequentially combined into single-feature vectors with lengths of  $N \times 2125$ . For the classification of elbow fracture, the suggested method has a kappa value of 0.943% and an accuracy of 97.1%.

Rashid et al.<sup>[22]</sup> deliberated the Deep CNN and long short-term memory (DCNN-LSTM) to Identify Human Wrist Fractures. To address the issue of class imbalance, this framework employs data augmentation to generate a rotated oversample of imageries for minority classes during training. A 28-layer dilated CNN (DCNN) is fed with pre-processed and augmented standardized imageries to extract deep, valuable features. After that, the suggested LSTM network is given deep features to differentiate between normal and wrist fractures.

The study<sup>[23]</sup> suggests a paradigm for sentiment analysis that uses hybridized neural networks and a modified word frequency-inverse document frequency method. Following data preprocessing, a non-linear global weighting factor is included to enhance the basic term frequency-inverse document frequency scheme. This improved methodology combines the k-best selection method to vectorize textual characteristics. After that, the convolutional neural network and long short-term memory that comprise the deep neural network get embedded features. It is compared to multiple state-of-the-art baseline models across several performance indicators and datasets to show how effective the proposed model is.

After preliminary data processing, the study<sup>[24]</sup> suggests a Hybridised Deep Neural Network-based framework for sentiment analysis to optimize feature space with the help of sentiment information extracted using our specially developed SentiWordNet lexicon-linked fitness function. It achieved this by modifying the dispersive fly optimization by adjusting its neighbour counterpart and then applying Neighbour Adjusted Dispersive fly optimization. This change aids in evading the local ideal solution and bolsters the optimization process so it may more effectively approach the global optimal solution. The proposed hybrid approach is compared to several state-of-the-art approaches using a range of performance measures to prove its efficacy.

The investigation shows numerous issues with prevailing methods in reaching great precision, sensitivity, specificity, and low error rates. Hence, this study proposes the Deep Convolutional Neural Network-based Distal Radius Fracture Classification Model (DCNN-DRFCM) to diagnose DRFs using anteroposterior and lateral wrist radiographs.

### **3. Deep neural network-based distal radius fracture classification model (DNN-DRFCM)**

One of the most frequent types of fractures, distal radius fractures, may happen to younger persons due to high-energy trauma or to older adults due to low-energy trauma. Untreated fractures may progress to degenerative diseases; therefore, getting them treated properly is essential. In adults, almost 20% of fractures are distal radial fractures (DRF). The gold standard for diagnosing DRFs is still plain radiography. In an

outpatient clinic or emergency department, non-orthopaedic surgeons may be the main doctors who examine fractures, and since DRF is sometimes subtle, the fracture could pass undetected. Subsequent problems, including malunion and osteoarthritis, may develop from untreated fractures. Consequently, there is a need for a better way to identify fractures quickly and accurately. Automated fracture diagnosis in various anatomical areas has lately seen impressive advancements using deep learning-based systems (DLS). This includes the lower and upper extremities, including the elbow, foot, knee, shoulder, ankle, femur, pelvis, humerus, tibia and hip. An area of machine learning, deep learning, investigates how an artificial system may learn from its own experiences (e.g., input data or feedback) and perform better at any given task over time without being explicitly programmed. We should train a CNN classification model to identify wrist fractures from anteroposterior and lateral radiographs and then use the model to diagnose the fracture autonomously. This study proposes the Deep Convolutional Neural Network-based Distal Radius Fracture Classification Model (DCNN-DRFCM) to diagnose DRFs using anteroposterior and lateral wrist radiographs.

**Figure 1** shows the radiographic image samples from the dataset used in this research. The normal angle of radial inclination is  $15^{\circ}$  to  $25^{\circ}$ . An impaction fracture in the metaphysis of the distal radius might explain the abnormal angle. There are other parameters like the ulnar variance, ulnar height, and dorsal distal radius inclination to diagnose fractures. The comprehension of the relationship between radiographic findings and clinical outcomes is still lacking. The surgeon may have greater clarity of the fracture and its reduction if they are familiar with the radiographic landmarks, parameters, and damage patterns.

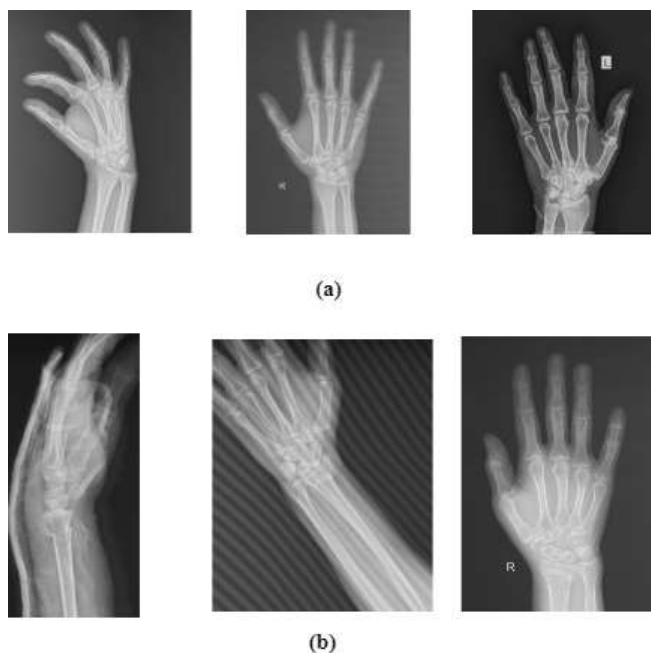


**Figure 1.** Radiographic image samples from the dataset used in this research (a) normal; (b) abnormal images.

**Figure 2** shows the proposed DCNN-DRFCM model. The Saveetha Medical College Hospital’s image archiving and communication system was used to retrieve 100 radiographic images of the wrist<sup>[25]</sup>. The method is error-sensitive if imageries are captured in unaware conditions or have unpredicted noise added to them. Before any blocks were applied, the data received pre-processing employing normalization. Global contrast normalization with initial clipping was performed after reading each radiograph in this investigation. Among the several subfields of DL, CNN-based feature extraction models have consistently outperformed the competition in an extensive range of inspection tasks. Image resolution and feature specifics are major factors in determining the hyper-parameters for feature extraction methods. So, to automatically extract the fracture trace map from tumble tunnel wrist images, it is required to rearrange the current CNN-based methods with well-stated application criteria, considering the intricacy of feature extraction and the

carefulness of the fracture trace. This work assessed how well the CNN classification algorithm could identify DRFs from lateral and anteroposterior wrist radiographs. A deep-learning model for accurate distal radius fracture identification was developed in this work using pixel-level fracture annotations. Object detection networks provide more useful information than classification networks by identifying where the fracture is.

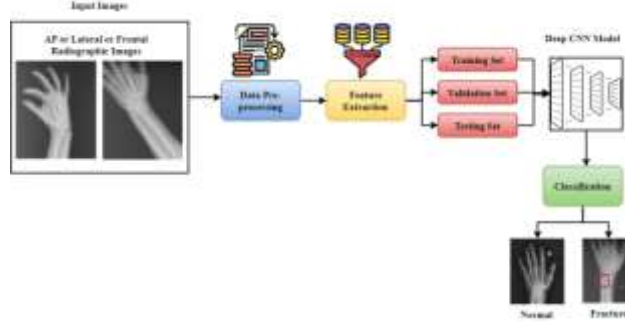


**Figure 2.** Proposed DCNN-DRFCM model.

The fracture line, which represents the texture data from the medical image, allows the doctor to assess the fracture. This work improves the picture texture information and then uses ResNet to identify fractures and non-fractures. One may apply the Sobel, Laplace, Gabor, or Schmid filters on an image’s texture. According to our experimental validation, the Schmid filter outperforms all others when identifying fractures. The rotation invariance of the Schmid filter allows it to capture the description of the invariant texture. For photographs of bones, the Schmid filter can characterize fracture lines and their margins. The kernel function is primarily responsible for generating the transform matrix in a Schmid filter, which is then used to perform the convolution operation on the fixed matrix. The following is the function of its kernel:

$$F(r, \rho, \tau) = \cos\left(\frac{2\pi\tau r}{\rho}\right) e^{-\frac{r^2}{2\rho^2}}, \quad r = \sqrt{x^2 + y^2} \quad (1)$$

As shown in Equation (1), where  $\rho$  denotes the standard deviation of the Gaussian,  $\tau$  indicates the number of cycles of the harmonic function within Gaussian envelopes of the filters, and  $(x, y)$  signifies the coordinate position of pixel point.

**Figure 3** shows the DCNN model for distal radius fracture classification. The DCNN model included convolutional layers, input layers, region of interest (ROI) layers, feature map layers, classifier, pooling, and output layers. ROI pooling is used to classify the input images and establish the needed area based on the location of interest. At each sliding window, the proposal’s area is anticipated. The next step is to forecast the bounding box’s offset value. Compared to previous networks, this one is faster and more efficient in detecting risks. The initial layer of the suggested model is the input layers, which accepts the X-ray images of the dimensions  $Q \times P$  and automatically convert them into  $N \times M$ . The X-ray images are garnered to particular sizes and fed to convolutional layers. A received image is convolved with a kernel of a certain size in the convolutional layer. A default arrangement is included in the proposed model. Reducing the effort and processing cost of the model, the convolution layer reduces the size of the input X-ray picture. Examining Equation (2) reveals the size of the convolution layer.

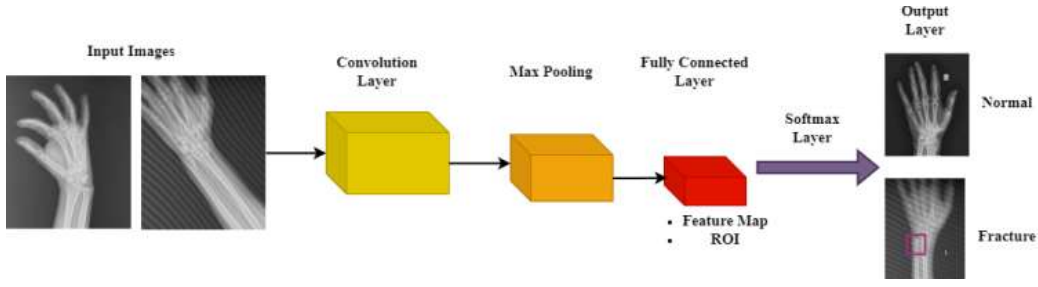


**Figure 3.** DCNN model for distal radius fracture classification.

$$Output\ Size = \frac{(j - l) + 1}{w} \quad (2)$$

As inferred from Equation (2), where  $j$  indicates the input dimensions,  $l$  denotes the kernel dimensions, and  $w$  is the stride dimensions.

The pooling layer performs down-sampling on the X-ray images to facilitate additional input to the subsequent layer. For optimal results, the model used max-pooling across the board. Here is the output of the pooling layer, as described in Equation (3).

$$Output\ Size = \frac{(j - q) + 1}{w} \quad (3)$$

As found in Equation (3), where  $j$  denotes the input dimensions,  $q$  indicates the pooling dimensions, and  $w$  signifies stride sizes. The suggested study uses ReLu as an activation function; unlike other activation functions, its gradients are either 0 or 1, and it disregards negative values. This allows for much quicker computing. The Equation (4) is used to display the ReLu activation function.

$$x = \max(0, y) \quad (4)$$

With the fracture locations preserved, the feature maps provide comprehensive X-ray image data. If, for example, an X-ray picture shows fractures on the right sides, the activation of convolutional layers will cause the fractures to appear on the right side of the resulting feature map, which incorporates all features from the input image.

Layers of fully connected neural networks using a Softmax classifier followed the convolutional layer. Softmax classifiers form the output layers as an extension of the logistic and normalized exponential functions. These classifiers take  $K$ -dimensional vectors of arbitrary real value and transform them into  $K$ -dimensional vectors of real value in ranges  $(0, 1)$  that add up to one for specificity analysis. The following Equation (5) gives the function:

$$(X = j|y, S, a) = softmax_j(S_y + a) = \frac{e^{S_j y + a_j}}{\sum_i e^{S_j y + a_j}} \quad (5)$$

The model's interpretation was the class with the largest probability, and the output of the Softmax layers was the conditional likelihood distributions across the two target classes.

Equation (6) defines a cross-entropy loss function that may be used to calculate the discrepancy between the feature map forecasted by the DCNN model and the manually annotated fracture trace maps for sensitivity analysis:

$$L = - \sum_{j \in H+} s_0 \log Qr(Q_j = 1) - \sum_{j \in H-} s_1 \log Qr(Q_j = 0) \quad (6)$$

As shown in Equation (6), where  $s_0$  and  $s_1$  are the loss weight of the fractures and non-fractures classification,  $Qr(Q_j)$  denotes the likelihood distribution of the predicted feature maps, and  $H +$  and  $H -$  represent the non-fracture pixel and the fracture pixel of input images, correspondingly. Every convolutional

layer produces forecast feature maps and respective side-outputs loss labelled  $L_{side-output}^j$ , where  $j$  is layer numbers. The side-output layer is concatenating to the last fused maps, which creates the fused loss-labelled  $L_{fused}$ . The total cross-entropy loss functions are determined by adding the loss values of the fused map and the convolutional layer as in Equation (7) for the predicted error rate:

$$L_{overall} = \sum L_{side-output}^j + L_{fused} \quad (7)$$

Before beginning the training process, the following first model hyper-parameter must be set: number of epochs, learning rate, batch size, momentum, and weight decay. The number of photos used to train the target model is called the batch size. The learning rate is how often the optimization algorithm updates the network weights. The loss function's regularization term has a coefficient called weight decay. In the stochastic gradient descent (SGD) process, momentum regulates the model's convergence rate. Every time a network receives all the data needed for a forward computation and backpropagation, it is called an epoch. To achieve optimal performance, it is recommended to modify the number of epochs to prevent overfitting or underfitting.

**Algorithm 1** shows the fracture detection algorithm based on the DCNN model. This study has incorporated data augmentation (DA) and transfer learning (TL) techniques to enhance CNN's predictive ability. The data augmentation can solve the issue of insufficient data for model training. The zooming technique is used on the original image data to expand the data amount to produce images with a similar label. TL models are used mostly for image classification-related problems. The proposed DCNN model has been confirmed concerning hyper-parameters such as optimizer SGD and ADAM with a learning rate of 0.01, several epochs of 100, and batch size of 120. The 70% of data for training and 30% for the testing of the model has been used for both data sets (real and augmented). The proposed DCNN-DRFCM model increases the specificity, classification accuracy, F1-score ratio, sensitivity, and reduced error rate compared to existing approaches.

---

**Algorithm 1** Fracture Detection Algorithm based on the DCNN model

---

- 1: Input: Labeled Training Data  $Y, M$  is total training data. For  $Y_j$  there is an original X-ray image and an annotated binary mask,  $Y_j = img_j, mask_j$
  - 2: Output  $X = \{X_1, X_2, \dots, X_M\}$ ,  $X_j$  is the X-ray image with detection bounding boxes.
  - 3: Load  $Y$  from the training dataset
  - 4: **for**  $l = 1, \dots, epoch\_max$  **do**
  - 5:   **for** local epoch  $\leftarrow 1$  to  $E$  **do**
  - 6:     Optimize the hyperparameters
  - 7:   **End**
  - 8: **End**
  - 9: Update model parameters
  - 10: **Return**
- 

## 4. Results and discussion

This study proposes the Deep Convolutional Neural Network-based Distal Radius Fracture Classification Model (DCNN-DRFCM) to diagnose DRFs utilizing lateral and anteroposterior wrist radiographs. The Saveetha Medical College Hospital's image archiving and communication system was used to retrieve 100 radiographic images of the wrist<sup>[25]</sup>. Radiologists used bounding boxes to label all fractures and bones. The dataset was divided into a validation set of 10% and a training set of 90% to train fracture localization techniques for lateral and anteroposterior images.

The process of organizing and managing data at every stage of its lifespan is known as data curation. Data identification, description, preservation, transformation, and use are all part of its characteristics. Data curation services are used to ensure data is trustworthy, easily discoverable, compatible with other systems, and interoperable. Organizations risk never realizing their data's full potential without efficient data curation.

Data curation systematically organizes, manages, and enriches data to guarantee accessibility, relevance, and quality. Data curation entails structuring and integrating information gathered from many sources. It entails annotating, publishing, and presenting the data in a way that maintains its worth and makes it accessible for future use and preservation. An unsupervised machine learning technique, which involves clustering phrases according to their similarity, is crucial to active annotation because it allows the organization of training data to propose annotation labels to human annotators. By using active annotation, human annotators—often medical experts—can concentrate on challenging, untrustworthy medical claims. Furthermore, our strategy drastically cuts down on the cognitively costly process of context switching as the annotators handle groups of sentences with comparable semantic content. The annotators are ultimately responsible for determining the data’s labels.

All of the experiments in this research use cross-validation to provide the most accurate evaluations possible. The performance of the recommended DCNN-DRFCM model has been analyzed based on metrics like F1 score, sensitivity, classification accuracy, error rate and specificity compared with existing wrist fracture detection-combo (WFD-C)<sup>[18]</sup>, Deep Supervised Learning (DSL)<sup>[20]</sup>, Hand-Crafted and Deep Feature Fusion and Selection and Wolf Optimization Algorithm (HC-DFFS-WOA)<sup>[21]</sup>, Deep CNN and long short-term memory (DCNN-LSTM)<sup>[22]</sup>. **Table 1** demonstrates the experimental setup.

**Table 1.** Experimental setup.

Parameter	Value
Learning Rate	0.01
Filter Size	15
Activation Function	ReLU
The number of Feature Map	10 to 200
The number of input vector	128
Maximum epochs	5000
Pooling Size	3
The number of Input Channel	6
The probability of dropout	0.7

#### 1) Classification Accuracy Ratio

Treatment efficacy and patient care depend on accurate fracture classification from medical imaging, especially wrist X-rays. Because fracture skeleton maps are created by skeletonizing fracture trace maps, this research assesses the accuracy of pixel-level fracture feature extraction. Feature extraction from images is made efficient using a lightweight CNN architecture. To accurately diagnose fractures, deep-learning classifiers are given these extracted features.

$$Accuracy = \frac{TP + TN}{TP + FP + TN + FN} \quad (8)$$

As shown in Equation (8), where TP indicates True Positive (Recognized Properly), TN represents True Negative (Recognized Wrongly), FP symbolizes False Positive ( Disallowed Properly), and FN indicates False Negative ( Disallowed Wrongly). **Figure 4** shows the classification accuracy rate.

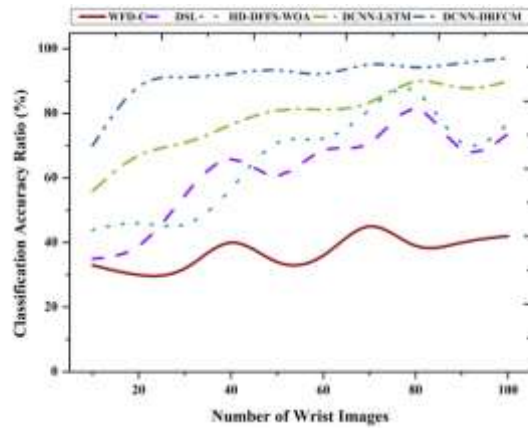


Figure 4. Classification accuracy ratio.

## 2) Sensitivity Ratio

To optimize the proposed model, it is important to include factors such as the cost of positive and negative misdiagnoses at both the individual and population levels. As with BoneView, substantially trained models like this need to deliberately balance sensitivity and specificity within the context of their intended purpose. With 95% confidence intervals, this study could evaluate the sensitivity, specificity, area under the receiver operating characteristics curves, and negative and positive predictive values. The model's accurateness in forecasting negative and positive results would be assessed by re-examining the initial radiography images. In addition, the research found that the DCNN could identify a rather visible fracture on the test set, even though the network is generally fairly sensitive. Based on Equation (6), the sensitivity ratio has been identified. **Figure 5** shows the sensitivity rate.

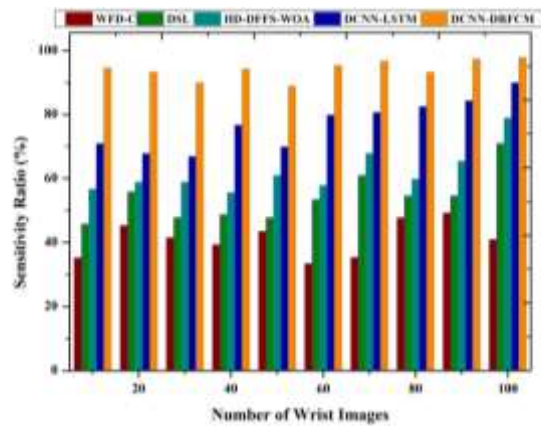
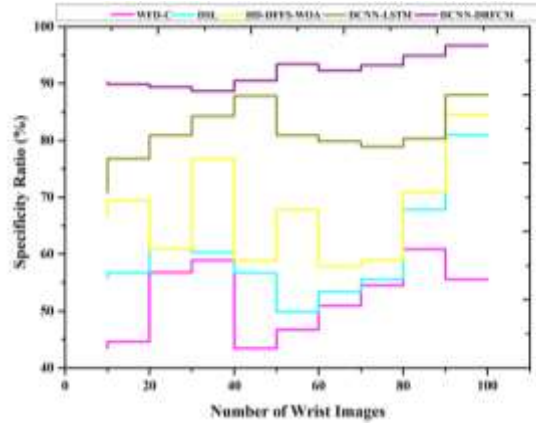


Figure 5. Sensitivity ratio.

## 3) Specificity Ratio

Deep learning CNN can learn features that discriminate between a growth plate and a fracture, as our findings indicate that there are minimal false-positive marks owing to growth plates on pediatric radiographs. Despite a general tendency toward reduced specificity for radiographs acquired with a cast on both lateral and anteroposterior images, this research did not find a statistically significant difference in network performance across fractures with and without casts. The reason for this may be the presence of cast-imposed linear artefacts that give the impression of fractures yet are just artefacts. According to this research, the anteroposterior and lateral views of fractures with little or no displacement were shown to be far less sensitive than fractures with substantial displacement. Because their identification relies on a small component of the overall image, slightly displaced fractures are inherently difficult to detect. Based on Equation (5), the specificity ratio has been identified. **Figure 6** shows the specificity ratio.



**Figure 6.** Specificity ratio.

#### 4) F1-Score Ratio

F1 score, precision, accuracy, and recall were the four assessment criteria used in the methods section. Both accuracy and recall are indicators of prediction quality; the latter shows the percentage of correctly diagnosed fractured instances, while the latter shows the proportion of incorrect predictions. Precision is the percentage of photos accurately predicted as having fractures as a percentage of all images. According to Equation (9), the F1 score is computed as the harmonic mean of recall and accuracy. This study averaged the accuracy, recall, and macro F1 score for 5-fold cross-validation. Accuracy was averaged over five folds to guarantee the findings' stability further. **Figure 7** demonstrates the F1-score ratio.

$$F1 - score = \frac{2 \times precision \times recall}{precision + recall} \quad (9)$$

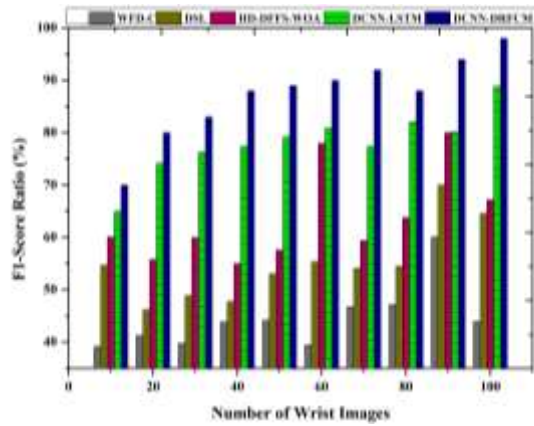


**Figure 7.** F1-Score ratio.

#### 5) Error Rate

Misdiagnosis of fractures, in particular, is prevalent in the emergency room due to the great volume of patients and the absence of time and sometimes resources for thorough examination. In the emergency department, numerous errors in interpreting images may be prevented if radiographs were either automatically processed or reviewed by a radiologist in real-time with AI support, aiding decision-making. In several experiments, this study monitored and simplified the learning rate to get the necessary minimal error value. It has a very accurate area under the curve (AUC) of 0.975 for fracture diagnosis. A 47% decrease in the diagnostic error rate among emergency department physicians was reportedly achieved with the use of this method. Out of all the reports, our program's data use for learning was the lowest, ranging from 100th to one-thousandth per cent. Based on Equation (7), the error rate has been predicted. **Figure 8** shows the error rate.

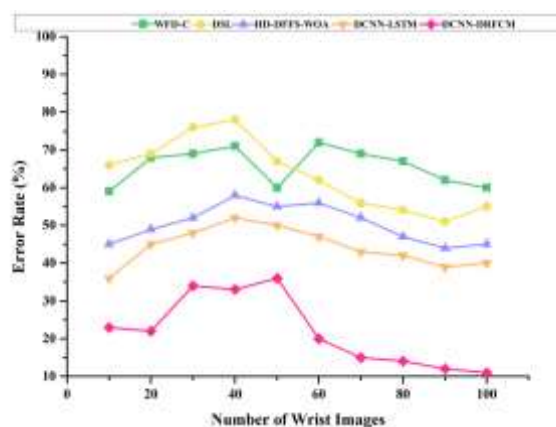


**Figure 8.** Error rate.

## 5. Conclusion

This work presents a new way to assess and classify the DRF using computational modelling and ML approaches; this might help create real-time patient-specific treatment and rehabilitation programs. This study proposes the Deep Convolutional Neural Network-based Distal Radius Fracture Classification Model (DCNN-DRFCM) to diagnose DRFs using lateral and anteroposterior wrist radiographs. Using deep learning to speed up computational modelling calculations is an exciting new direction. As rapidly as DL prediction accuracy is sufficient, it will be possible to employ simulation findings rapidly in healthcare practice environments. A deep CNN gathers and classifies the depth data from images depicting DRF. The numerical findings demonstrate that the recommended model enhances the specificity rate of 97.8%, classification accuracy rate of 99.3%, F1-score rate of 95.6%, sensitivity ratio of 96.5%, and decreases the error rate of 11.2% than other popular approaches. The network was trained using a smaller dataset compared to the X-ray image computer vision identification, which may range from thousands of original images to hundreds of thousands. Future studies will identify the accurate location and size of the fracture and explore the study's potential relevance to other long bones of the arms and legs.

## Author contributions

Conceptualization, IM, AS, SM, CP, GC, MA and M; methodology, IM, AS and SM; software, CP, GC, MA and M; validation, IM, AS and SM; formal analysis, CP, GC, MA and M; investigation, AS, SM and CP; resources, GC, MA and M; data curation, IM, AS and SM; writing—original draft preparation, IM, AS, SM, CP, GC and MA; writing—review and editing, IM, AS and SM. All authors have read and agreed to the published version of the manuscript.

## Conflict of interest

The authors declare no conflict of interest.

## References

1. Chung KC, Kim HM, Malay S, et al. Comparison of 24-month outcomes after treatment for distal radius fracture: The WRIST randomized clinical trial: The WRIST randomized clinical trial. *JAMA Netw. Open.* 2021; 4(6): e2112710.
2. Fares AB, Childs BR, Polmear MM, et al. Dorsal Bridge Plate for Distal Radius Fractures: A Systematic Review. *The Journal of Hand Surgery.* 2021; 46(7): 627.e1-627.e8. doi: 10.1016/j.jhsa.2020.11.026
3. Forde C, Nicolson PJ, Vye C, et al. Lower limb muscle strength and balance in older adults with a distal radius fracture: a systematic review. *BMC Musculoskeletal Disorders.* 2023; 24(1). doi: 10.1186/s12891-023-06711-4
4. Dutton LK, Rhee PC. Complex Regional Pain Syndrome and Distal Radius Fracture. *Hand Clinics.* 2021; 37(2): 315-322. doi: 10.1016/j.hcl.2021.02.013

5. Shen O, Chen CT, Jupiter JB, et al. Functional outcomes and complications after treatment of distal radius fracture in patients sixty years and over: A systematic review and network meta-analysis. *Injury*. 2023; 54(7): 110767. doi: 10.1016/j.injury.2023.04.054
6. Greig D, Silva M. Management of Distal Radius Fractures in Adolescent Patients. *Journal of Pediatric Orthopaedics*. 2021; 41(Suppl 1): S1-S5. doi: 10.1097/bpo.0000000000001778
7. Abitbol A, Merlini L, Masméjean EH, et al. Applying the WALANT technique to surgical treatment of distal radius fractures. *Hand Surgery and Rehabilitation*. 2021; 40(3): 277-282. doi: 10.1016/j.hansur.2021.02.001
8. Gutiérrez-Espinoza H, Araya-Quintanilla F, Olgún-Huerta C, et al. Effectiveness of surgical versus conservative treatment of distal radius fractures in elderly patients: A systematic review and meta-analysis. *Orthopaedics & Traumatology: Surgery & Research*. 2022; 108(5): 103323. doi: 10.1016/j.otsr.2022.103323
9. Belloti JC, Alves BVP, Faloppa F, et al. The malunion of distal radius fracture: Corrective osteotomy through planning with prototyping in 3D printing. *Injury*. 2021; 52: S44-S48. doi: 10.1016/j.injury.2021.05.048
10. Liu X, Miramini S, Patel M, et al. Development of numerical model-based machine learning algorithms for different healing stages of distal radius fracture healing. *Computer Methods and Programs in Biomedicine*. 2023; 233: 107464. doi: 10.1016/j.cmpb.2023.107464
11. Suzuki T, Maki S, Yamazaki T, et al. Detecting Distal Radial Fractures from Wrist Radiographs Using a Deep Convolutional Neural Network with an Accuracy Comparable to Hand Orthopedic Surgeons. *Journal of Digital Imaging*. 2021; 35(1): 39-46. doi: 10.1007/s10278-021-00519-1
12. Tanzi L, Vezzetti E, Moreno R, et al. X-Ray Bone Fracture Classification Using Deep Learning: A Baseline for Designing a Reliable Approach. *Applied Sciences*. 2020; 10(4): 1507. doi: 10.3390/app10041507
13. Raisuddin AM, Vaattovaara E, Nevalainen M, et al. Critical evaluation of deep neural networks for wrist fracture detection. *Scientific Reports*. 2021; 11(1). doi: 10.1038/s41598-021-85570-2
14. Sequeira SB, Grainger ML, Mitchell AM, et al. Machine Learning Improves Functional Upper Extremity Use Capture in Distal Radius Fracture Patients. *Plastic and Reconstructive Surgery - Global Open*. 2022; 10(8): e4472. doi: 10.1097/gox.0000000000004472
15. Dupuis M, Delbos L, Veil R, et al. External validation of a commercially available deep learning algorithm for fracture detection in children. *Diagnostic and Interventional Imaging*. 2022; 103(3): 151-159. doi: 10.1016/j.diii.2021.10.007
16. Ren M, Yi PH. Deep learning detection of subtle fractures using staged algorithms to mimic radiologist search pattern. *Skeletal Radiology*. 2021; 51(2): 345-353. doi: 10.1007/s00256-021-03739-2
17. Yang F, Cong R, Xing M, et al. Study on AO classification of distal radius fractures based on multi-feature fusion. *Journal of Physics: Conference Series*. 2021; 1800(1): 012006. doi: 10.1088/1742-6596/1800/1/012006
18. Hardalaç F, Uysal F, Peker O, et al. Fracture Detection in Wrist X-ray Images Using Deep Learning-Based Object Detection Models. *Sensors*. 2022; 22(3): 1285. doi: 10.3390/s22031285
19. Hrzić F, Tschauer S, Sorantin E, et al. Fracture Recognition in Paediatric Wrist Radiographs: An Object Detection Approach. *Mathematics*. 2022; 10(16): 2939. doi: 10.3390/math10162939
20. Meena T, Roy S. Bone Fracture Detection Using Deep Supervised Learning from Radiological Images: A Paradigm Shift. *Diagnostics*. 2022; 12(10): 2420. doi: 10.3390/diagnostics12102420
21. Malik S, Amin J, Sharif M, et al. Fractured Elbow Classification Using Hand-Crafted and Deep Feature Fusion and Selection Based on Whale Optimization Approach. *Mathematics*. 2022; 10(18): 3291. doi: 10.3390/math10183291
22. Rashid T, Zia MS, Najam-ur-Rehman, et al. A Minority Class Balanced Approach Using the DCNN-LSTM Method to Detect Human Wrist Fracture. *Life*. 2023; 13(1): 133. doi: 10.3390/life13010133
23. Dey RK, Das AK. Modified term frequency-inverse document frequency based deep hybrid framework for sentiment analysis. *Multimedia Tools and Applications*. 2023; 82(21): 32967-32990. doi: 10.1007/s11042-023-14653-1
24. Dey RK, Das AK. Neighbour adjusted dispersive flies optimization based deep hybrid sentiment analysis framework. *Multimedia Tools and Applications*. Published online January 15, 2024. doi: 10.1007/s11042-023-17953-8
25. SMCH. Available online: <https://www.smc.saveetha.com/> (accessed on 20 February 2024).